

1 **A STUDY ON THE COST-EFFECTIVE METHODS FOR RECOVERY OF SKID**
2 **RESISTANCE ON CONCRETE PAVEMENT**

3
4
5
6 **Kazuhiro NAKAMURA, Corresponding Author**

7 NEXCO Research Institute Japan

8 1-4-1 Tadao, Machida-shi, Tokyo 194-8508 Japan

9 Tel: +81-42-791-1626 Fax: +81-42-791-2380; Email: k.nakamura.aj@ri-nexco.co.jp

10
11 **Daijiro MATSUMOTO**

12 West Nippon Expressway Company Limited

13 10-20 Cyuotyo Kawasaki-shi, Hyogo 666-0016 Japan

14 Tel: +81-72-768-8023; Email: d.matsumoto.aa@w-nexco.co.jp

15
16 **Masakazu SATO**

17 NEXCO Research Institute Japan

18 1-4-1 Tadao, Machida-shi, Tokyo 194-8508 Japan

19 Tel: +81-42-791-1626 Fax: +81-42-791-2380; Email: m.sato.au@ri-nexco.co.jp

20
21 **Keizo Kamiya**

22 NEXCO Research Institute Japan

23 1-4-1 Tadao, Machida-shi, Tokyo 194-8508 Japan

24 Tel: +81-42-791-1626 Fax: +81-42-791-2380; Email: k.kamiya.ab@ri-nexco.co.jp

25
26
27 Word count: 2,387 words text + 17 tables/figures x 250 words (each) = 6,637 words

28
29
30
31
32
33
34 Submission Date: November 7, 2014

1 ABSTRACT

2
3
4
5
6
7
8
9
10
11
12
13
14
15
16
17

Rapid reduction in skid resistance on concrete pavements inside tunnels has long been suffered all over Japan. As a result of comprehensive research and study on the expressways operated by NEXCO, it became clear that the decrease in skid resistance in tunnel sections is caused by the polishing action by vehicles' tires passing without water. It was also speculated that higher skid resistance can be sustained as with larger macro-texture, even after the texture is polished by vehicles passing. It was further confirmed that the shape of macro-texture also affects skid resistance; angular-shaped positive macro-texture assures higher resistance. Finally judging from the experiments on surface roughening methods for the skid resistance recovery on the concrete road surface, shot-blast with bigger steel balls was proved to be the most cost-effective way.

Keywords: Concrete Pavement, Skid Resistance, Texture, Recovery Method

1 INTRODUCTION

2
3 Needless to say, safety control is one of the most important assignments for road administrators. In
4 order to achieve this, Japanese nationwide toll expressway operators, NEXCO, have periodically
5 monitored skid resistance on the roadway. Most road surfaces provide sufficient skid resistance,
6 but some specific sections often face skid problems.

7
8 Figure 1 typifies skid resistance, μ_{80} (DFT) using dynamic friction tester at 80 km/hr (1) on the
9 cement concrete roadways in two survey sites with continuous tunnel-open sections. Both survey
10 sites A and B respectively indicate lower resistance in tunnel sections than open sections. This is
11 more remarkable on outer wheel path (OWP) areas, where vehicles' tires directly pass than
12 between wheel path (BWP) areas. In fact this phenomenon has been observed all over Japan and
13 long questioned among road administrators. Further more, although various surface roughening
14 efforts for improving skid concrete surface inside tunnels have been made, the once recovered skid
15 resistance will not be long lasting. As long as scientific reasons behind the fact are unknown, the
16 problem will remain. NEXCO Research Institute took the lead for solving the issue on behalf of
17 NEXCO.

18
19 This paper presents key findings through a series of comprehensive research and study, which
20 includes mechanism of the skid reduction, quantification of a problematic factor and suggestion on
21 practical recovery methods for sustaining skid resistance on the concrete road surface in tunnels.

22 23 24 MECHANISM OF THE DECREASE IN SKID RESISTANCE

25
26 As a first approach, micro-photographic and chemical studies were carried out. Photo 1 focuses on
27 cement paste parts of road surface enlarged by 5,000 times. The tunnel section's OWP image
28 seems shiny and polished-like, while the others show roughly jutting ones. According to
29 backscattered electron images 500-times enlarged cross sections of road surface in Photo 2, the
30 open section's surface contains more porosity as it pictures more dark colors. However, the other
31 tunnel section's photos appear massive structure with light colors (2).

32
33 Cement concrete samples taken from road surface were subjected to several chemical tests,
34 including CaO concentration test. Figure 2 contrasts the results between average of CaO
35 concentration and depth from the road surface. It clearly indicates lower CaO in open sections than
36 in tunnel sections. By further looking into atomic concentration of the road surface materials,
37 Figure 3 separates images of aggregates and cement paste parts, giving remarks for supporting the
38 above findings. Aggregates' texture in the open section's OWP is seemingly more roughly exposed
39 probably due to eroding cement paste parts on the roadway by rainfall. Meanwhile, the tunnel
40 section's images keep rather flat surface because of no rainwater. Its OWP provides the most flat
41 surface because passing vehicles' tires will polish without water. This is why Photo 1's center
42 picture looks polished-like.

43
44 In conclusion, rainfall will drain calcium of cement paste materials on the cement concrete road
45 surface in open sections, eventually enabling sustainable rough texture. In tunnel sections,
46 however, the surface texture is going to be polished and smooth by holding the cement pastes
47 especially on vehicles' wheel paths.

QUANTIFICATION OF PROFILE SHAPE

In response to the mechanism of decreasing skid resistance in tunnel sections, this chapter challenges how to quantify the slippery texture. The quantification is important as it can be followed by further finding an effective, longer sustainable countermeasure as a recovery method for skid resistance.

Figure 4 features the relation between $\mu_{80}(\text{DFT})$ and mean profile depth (MPD) using circular track meter (3) in advance of DFT on wheel path areas of road surface in tunnel sections. It is speculated that higher skid resistance can be sustained as with larger MPD or macro texture, even after the texture is polished by vehicles passing on the roadway.

Figures 5 and 6 respectively highlight surface profiles with an MPD level of around 1.0 at different spots. Both profiles here are already corrected to exclude even small undulation to every 8 digit sampling lengths (3). The profile shape in Figure 5 with lower $\mu_{80}(\text{DFT})$ is seemingly rounded at every peak and deep at every bottom. On the other hand, the higher friction group in Figure 6 shows angular shape at its peak points.

The shape of peak profiles needs to be quantified, as it is a direct contact to vehicles' tires and significantly affects skid resistance. Here is a new idea for quantification of profile peaks shape at an MPD or $\mu_{80}(\text{DFT})$ measurement site. As shown in Step 1 of Figure 7, the upper profile data exceeding zero are to be collected at every protruded group from A_1 to A_n . In every collected group A_n , Step 2 specifies that the profiles be plotted in the order of magnitude, and then a new line can be drawn between zero and the maximum profile value. In Step 3, the sum of the distances between the plotted profile and the new line can be obtained for each group. Finally the total summation of the distances from A_1 to A_n group can represent the quantified shape of peak profiles. This value is defined as below, namely hereafter, "Round Index".

$$\text{Round Index} = \sum_{n=1}^n dA_n \quad (1)$$

$$dA_n = \sum dni$$

where, dA_n : total distance for group A_n

dni : distance between profile and the new line at dni

The road surface macro texture's contribution to skid resistance is to be focused on its drainage ability and contact with a vehicle's tire (4). MPD represents the ability of draining water intervened between the tire and the road surface, and higher MPD can sooner drain the water. Meanwhile, when the texture is more angular with smaller round index, it can hold higher skid due to hysteresis.

Figure 8 demonstrates how MPD or macro texture and Round Index or profile shape can relate to $\mu_{80}(\text{DFT})$ on wheel path areas in tunnel sections. Marks "o" and "x" divide $\mu_{80}(\text{DFT})$ levels by

1 3.5, which is an average of all tunnel sections data in this study. The index generally well separates
2 the levels of skid resistance. The regression line also matches as a partition of the resistance. The
3 phenomenon can be supported by the past studies discussing factors such as texture, drainage and
4 contacts of tire and road surface, contributing to skid resistance (5) (6) (7) (8). It is speculated that
5 the lower the round index or the higher the angularity of profile shape, the higher the skid
6 resistance will be.

9 **EFFECTIVE SKID RESISTANCE RECOVERY METHOD**

10 Among many recovery methods for skid resistance on the surface of concrete pavement, surface
11 roughening methods were chosen, as they have been widely used on the NEXCO toll motorways.

13 **Preliminary Test**

14 Figure 9 relates MPD on roughly blasted specimen and compression strength of the concrete
15 material, as listed in Table 1. The MPD treated by shot-blasting method is more dependent on the
16 strength than that by water-jetting method. This is because the former earns texture by more
17 randomly brushing relatively weak part of cement mortar, while the latter gives so higher impulse
18 by water as to more entirely sweep cement mortar. Therefore the strength is considered important
19 to evaluate the characteristics of treatment methods. Mix number 2 in Table 1 was hereafter
20 adopted as its strength is the generally observed level in the field.

22 **Specimen Preparation**

23 In order to keep the level of flat surface on each specimen (50×50cm) in advance of skid-resistance
24 recovery testing, each material's surface was polished using a disk grinder, followed by using a
25 diamond wheeler, so that the test surface can be simulated in the slippery field. Table 2 lines up the
26 conditions of shot-blast (SB) and water-jet (WJ) methods for skid-resistance recovery. Moreover
27 diamond grinding (DG) method (9), which ditches longitudinally 3mm in width and 2mm in depth.
28 All the tests were conducted repectively using real machines after curing the specimen for about
29 one month. PHOTO 3 shows an example of SB machine's procedure.

31 **Skid Resistance Recovery Test**

32 Figure 10 relates $\mu_{80}(\text{DFT})$ and MPD values after all recovery tests for skid resistance. Skid
33 resistance of $\mu_{80}(\text{DFT})$ naturally tends to be higher as with the increase in MPD. The resistance of
34 materials with the same level of MPD is higher in the order of DG, SB and WJ.

35 Figure 11 depicts MPD and Round Index after the recovery tests. The regression line from Figure 8
36 was put here as a skid border. SB and DG data are plotted above the border line, so the two
37 methods are considered to give more effective textures than WJ method.

38 Among SB1, SB2 and SB3, the bigger the steel diameter, the higher both MPD and $\mu_{80}(\text{DFT})$
39 values. Use of bigger ball sizes under the same shot density will reduce the number of the balls,
40 making more random shots on the surface. Moreover, depth of texture will favorably increase as
41 heavy unit ball gives higher impulsive energy. Higher shot density SB4 shows slightly higher
42 MPD than SB2. This is considered due to increased shot areas deepening cement mortar.

43 Among WJ1 to WJ3 with a moving velocity of 2.0 meter/sec, MPD ranges only from 0.8 to 1.3
44 mm. Regardless of hydraulic pressure and sprinkling conditions, it seems difficult to recover to
45 higher MPD values. A slowly moving WJ4 shows the most remarkable improvement in MPD.

46 This is because of deepening the texture depth as well as narrowing the interval of ditches. But
47 WJ4 is the most costly in this test.

1
2
3 In summary, SB and DG methods will give more effective texture and higher skid resistance than
4 WJ method. Because the repair cost of SB is less expensive than WJ and DG, SB method is judged
5 the most cost effective.
6

7 **Cost Effective Method**

8 Finally, by taking into consideration cost factors, the most promising SB method can be selected.
9 Increasing shot density costs more than oversizing shot balls. In fact, double shot density almost
10 costs double, while ball size costs not that much. Therefore use of bigger ball size is highly
11 recommended as a cost-effective method. As this is expected to create long lasting texture, it can
12 be a sustainable recovery method for skid resistance of concrete road surface inside tunnels.
13

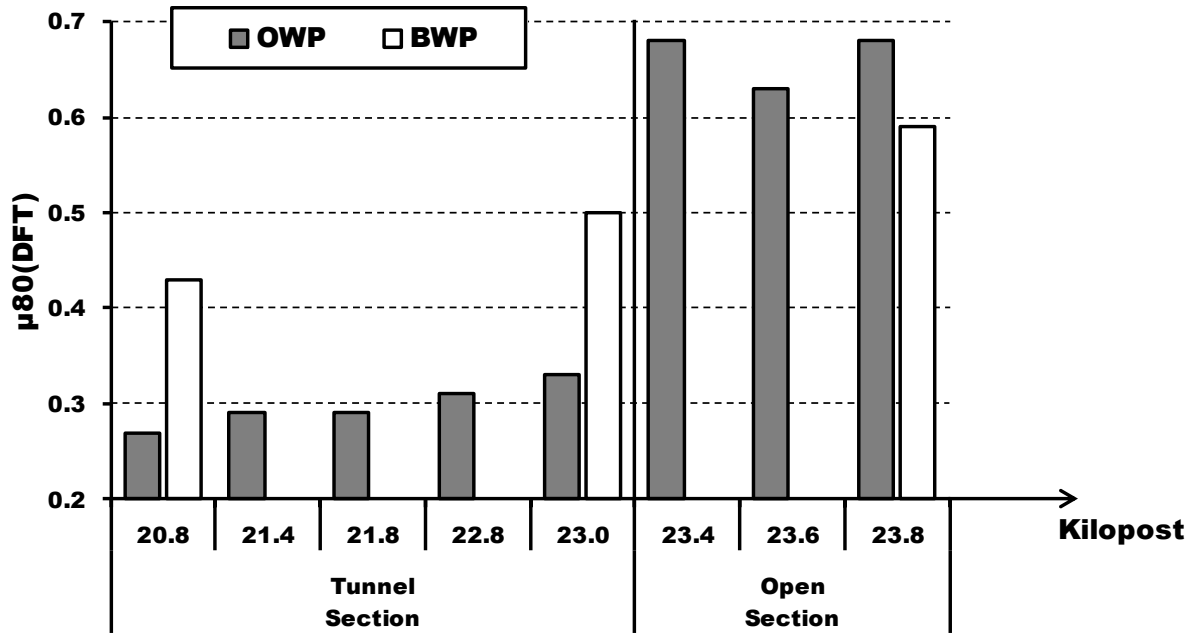
14 **CONCLUSION**

15
16
17 A series of comprehensive research and study was conducted for the purpose of understanding the
18 mechanism of fast reducing skid reduction in tunnel sections, quantification of a problematic
19 factor and finally suggestion on practical recovery methods for sustaining skid resistance. Here are
20 the findings as follows.
21

- 22 1. The road surface texture is going to be polished and smooth without water by holding the
23 cement pastes on vehicles' wheel paths.
- 24 2. Higher skid resistance can be sustained as with larger macro-texture, even after the texture is
25 polished by vehicles passing on the roadway.
- 26 3. Round index, which is newly defined in this paper, can quantify the roundness of profile shape
27 on the road surface.
- 28 4. It was confirmed that the lower the round index or the higher the angularity of profile shape,
29 the higher the skid resistance will be.
- 30 5. The strength of existing concrete material on the roadway is important to evaluate the
31 effectiveness of a surface roughening method of shot-blast.
- 32 6. Shot-blast and diamond-grinding methods are considered to give more effective textures than
33 water-jet method.
- 34 7. Shot-blast with bigger ball size is highly recommended as a sustainable skid resistance
35 recovery method on the concrete surface.

36
37 The authors believe the findings are all applicable not only in Japan but also any other country. It
38 would be highly appreciated if they are of help with road administrators who suffer skid problems
39 inside tunnels.
40
41

1



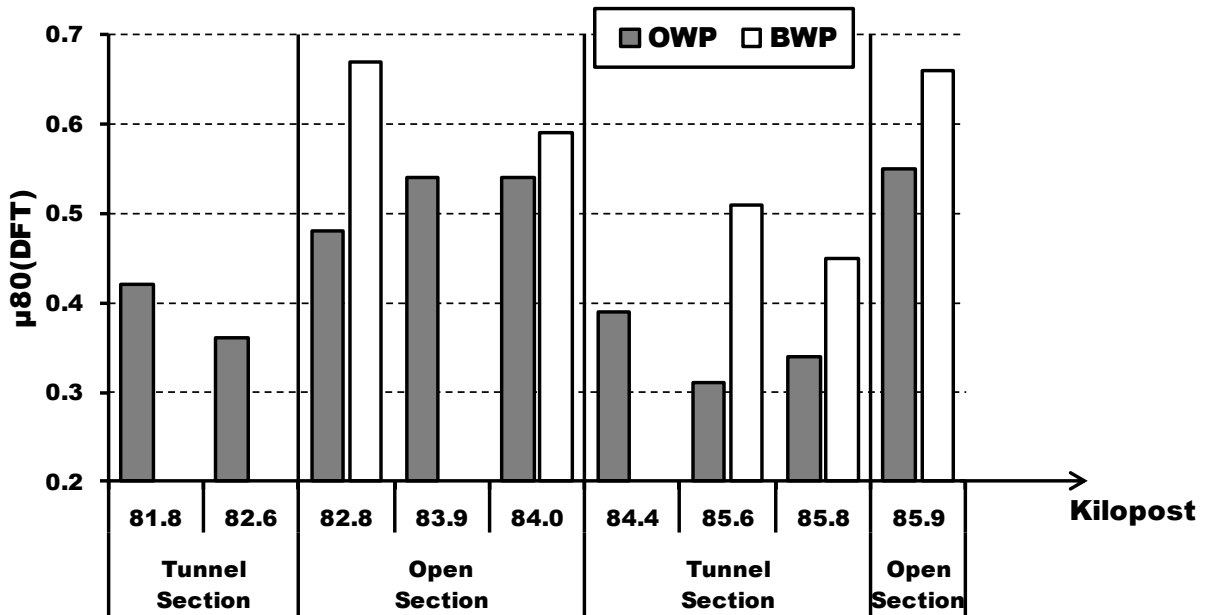
(a) Suvey site A (The Chubu region in Japan)

2

3

4

5



(b) Suvey site B (The Tohoku region in Japan)

6

7

8

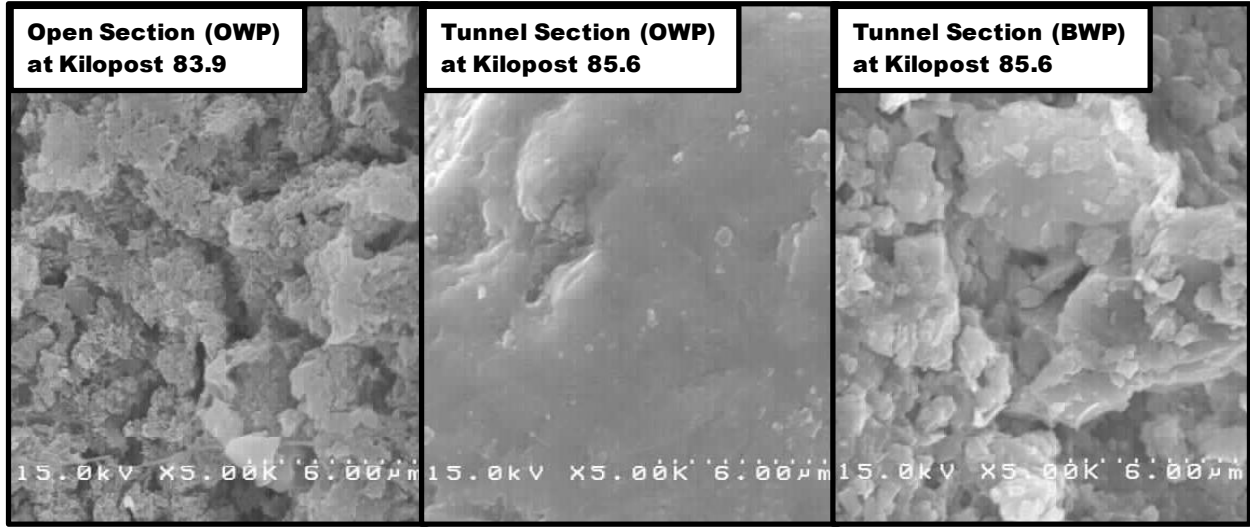
FIGURE 1 Skid resistance on cement concrete roadways

9

10

11

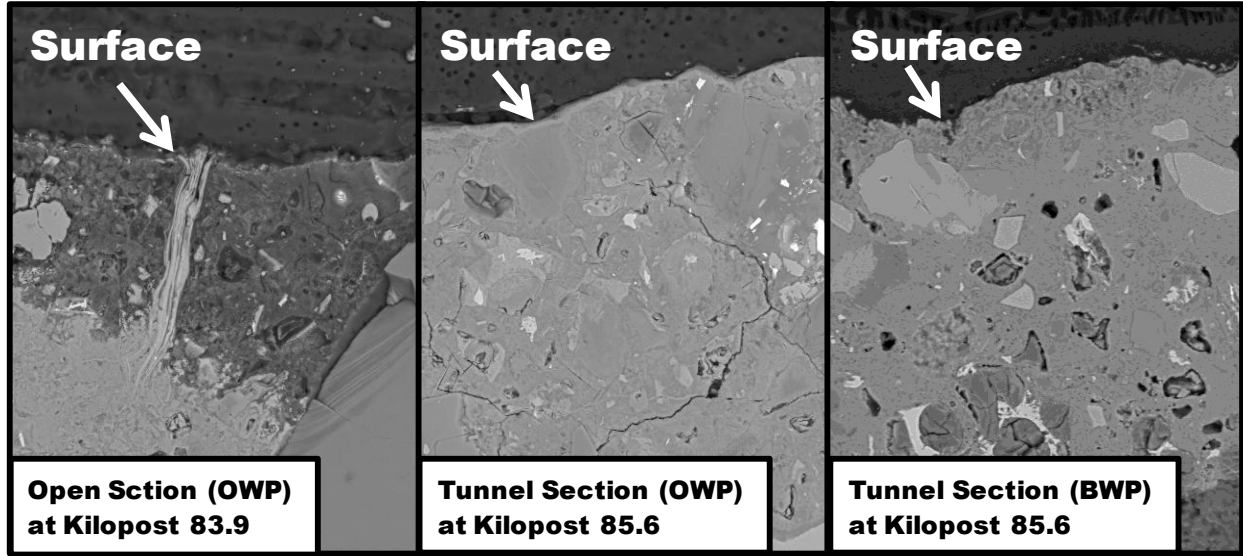
1



2
3
4
5
6

PHOTO 1 Focus on road surface (enlarged by 5,000 times) on Survey Site B

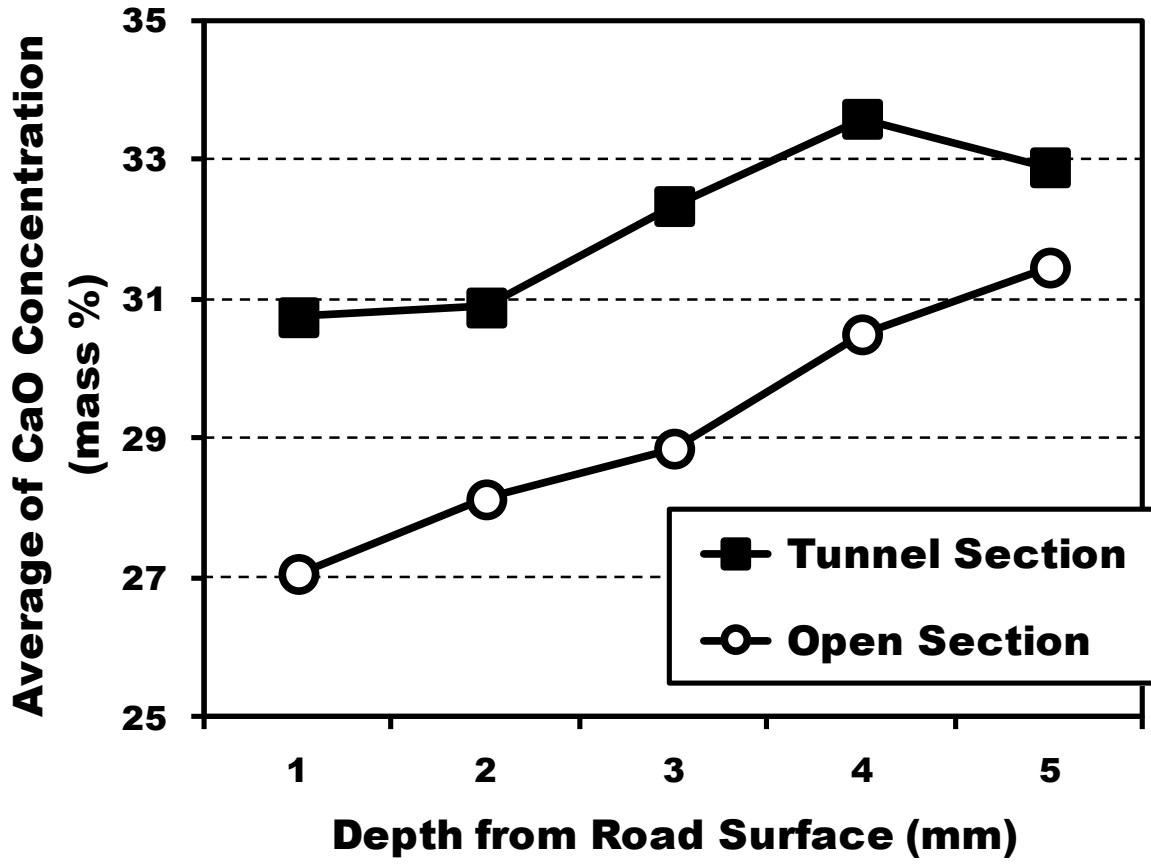
1



2
3
4
5
6

PHOTO 2 Cross sections of road surface (enlarged by 500 times) on Survey Site B

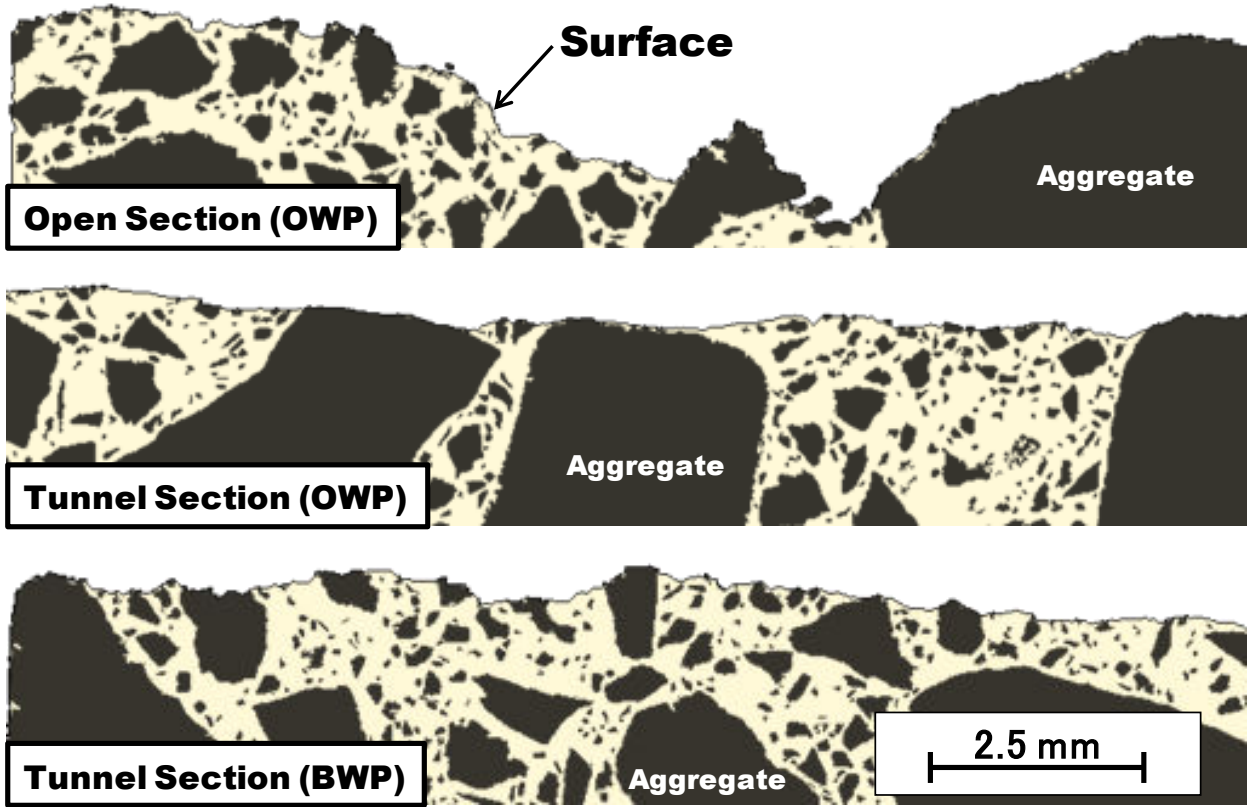
1



2
3
4
5
6

FIGURE 2 CaO concentration from road surface

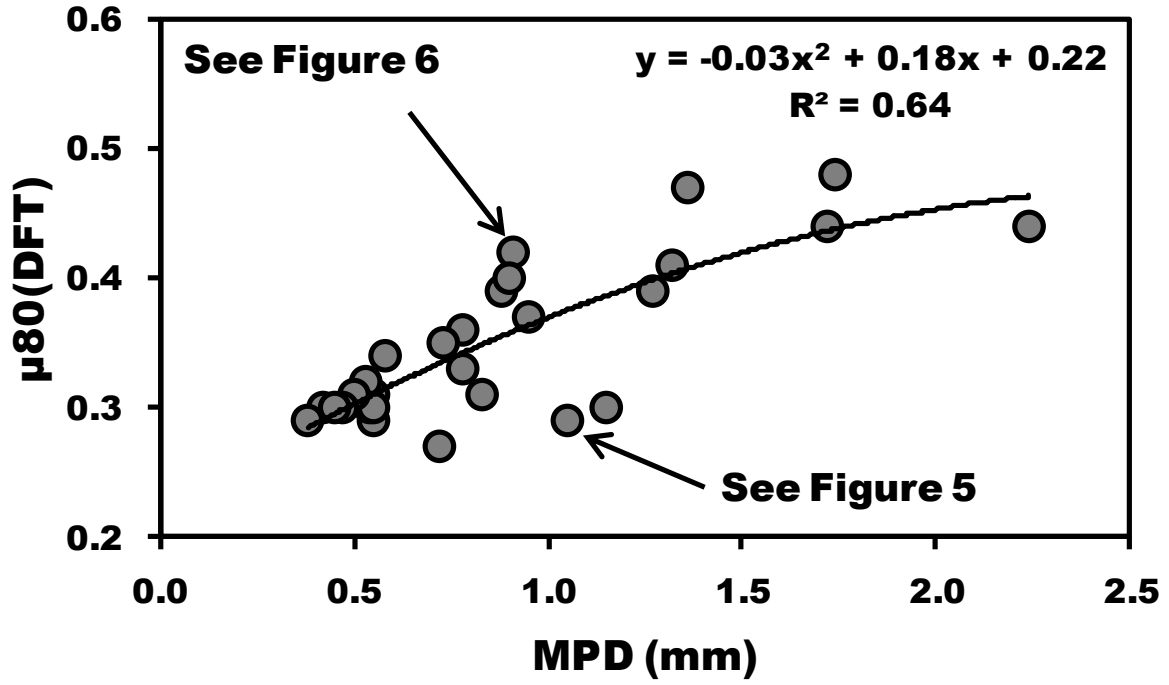
1



2
3
4
5
6

FIGURE 3 Images of aggregates and cement paste parts on concrete surface

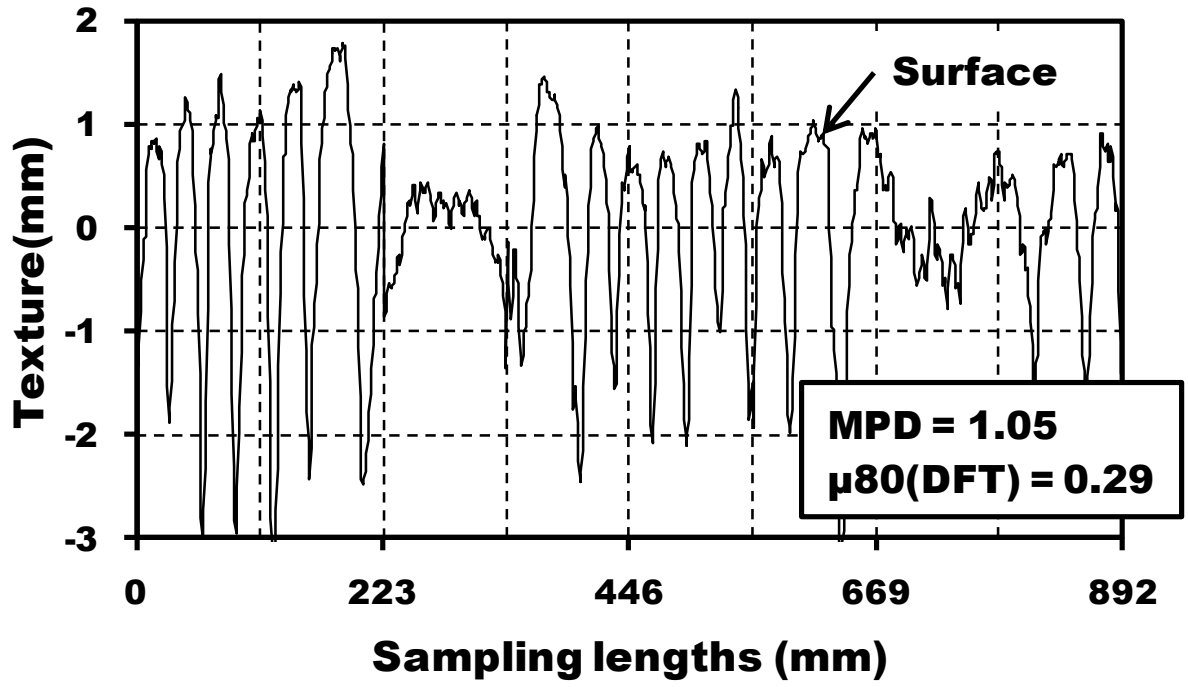
1



2
3
4
5
6

FIGURE 4 $\mu_{80}(\text{DFT})$ and MPD on OWP in tunnel sections

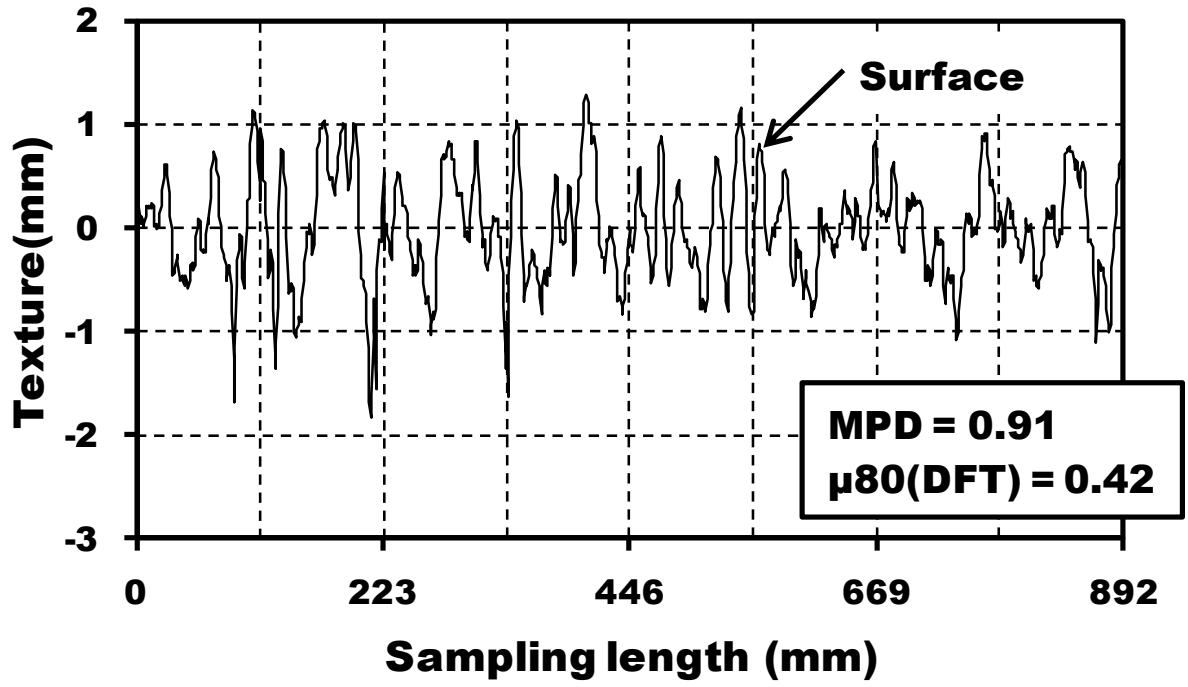
1



2
3
4
5
6

FIGURE 5 Surface profile with lower $\mu_{80}(\text{DFT})$

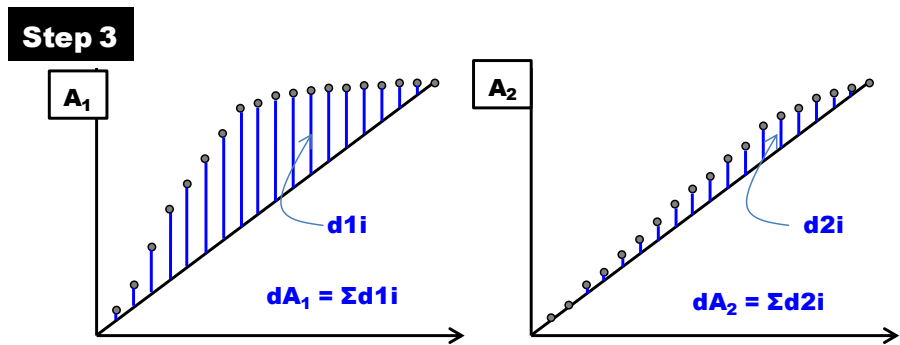
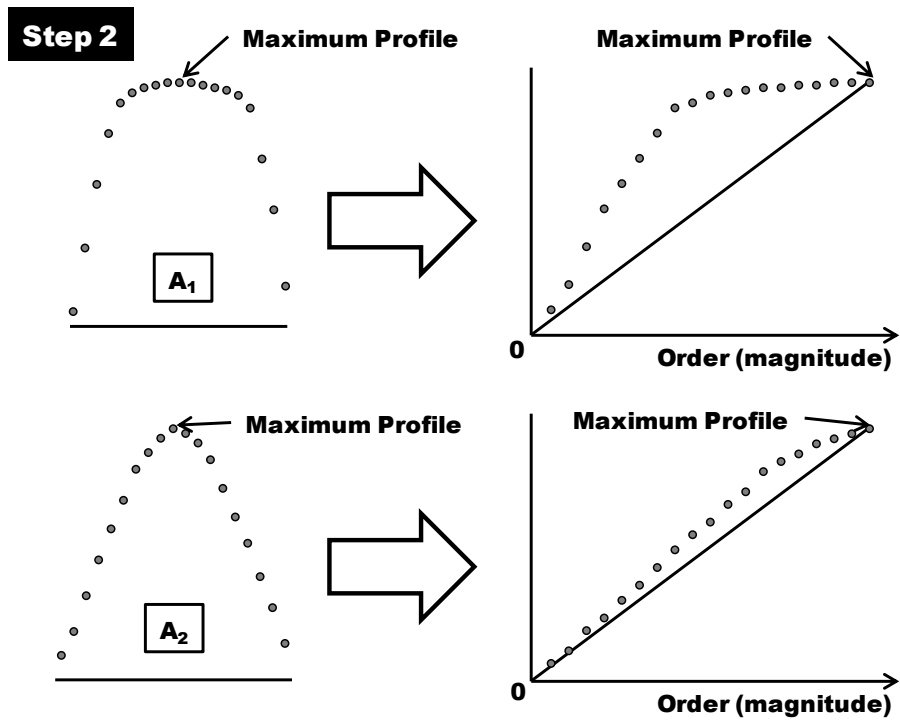
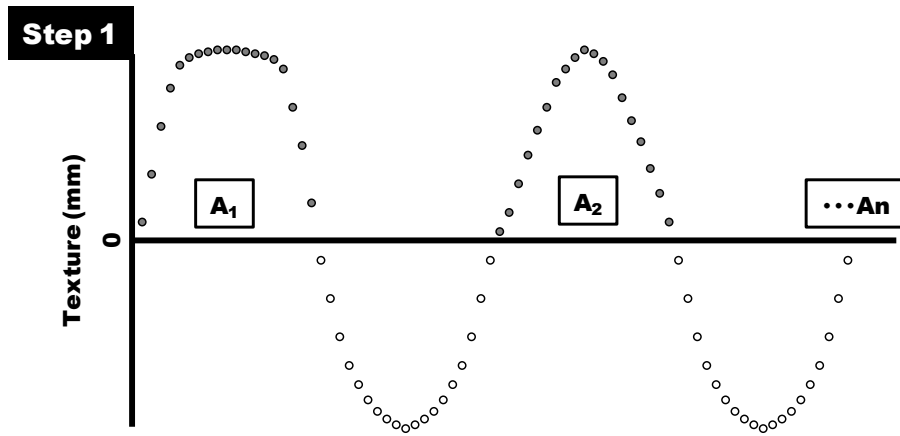
1



2
3
4
5
6

FIGURE 6 Surface profile with higher $\mu_{80}(\text{DFT})$

1



Round Index

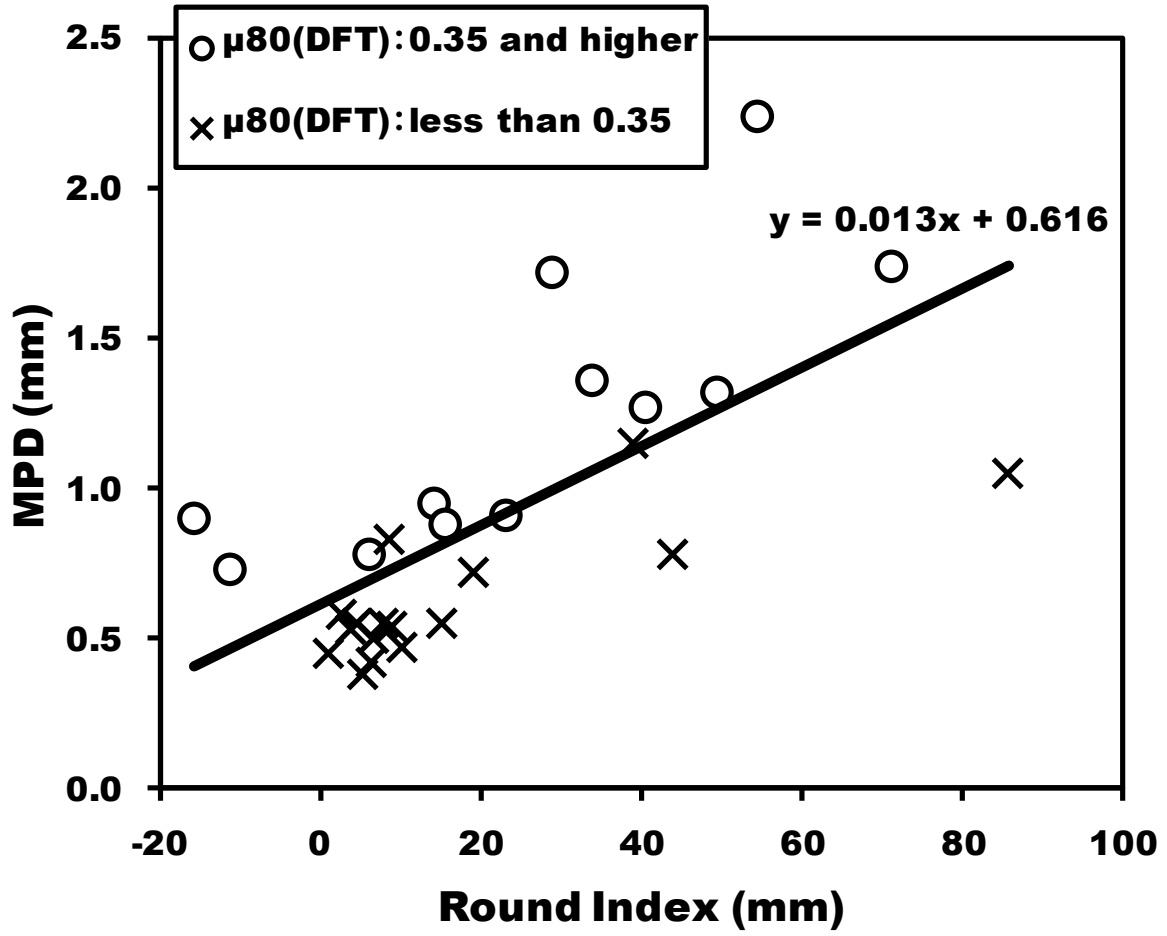
$$= \sum_{n=1}^n dA_n$$

$$dA_n = \sum d_n i$$

2
3
4
5

FIGURE 7 Calculation process of Round Index

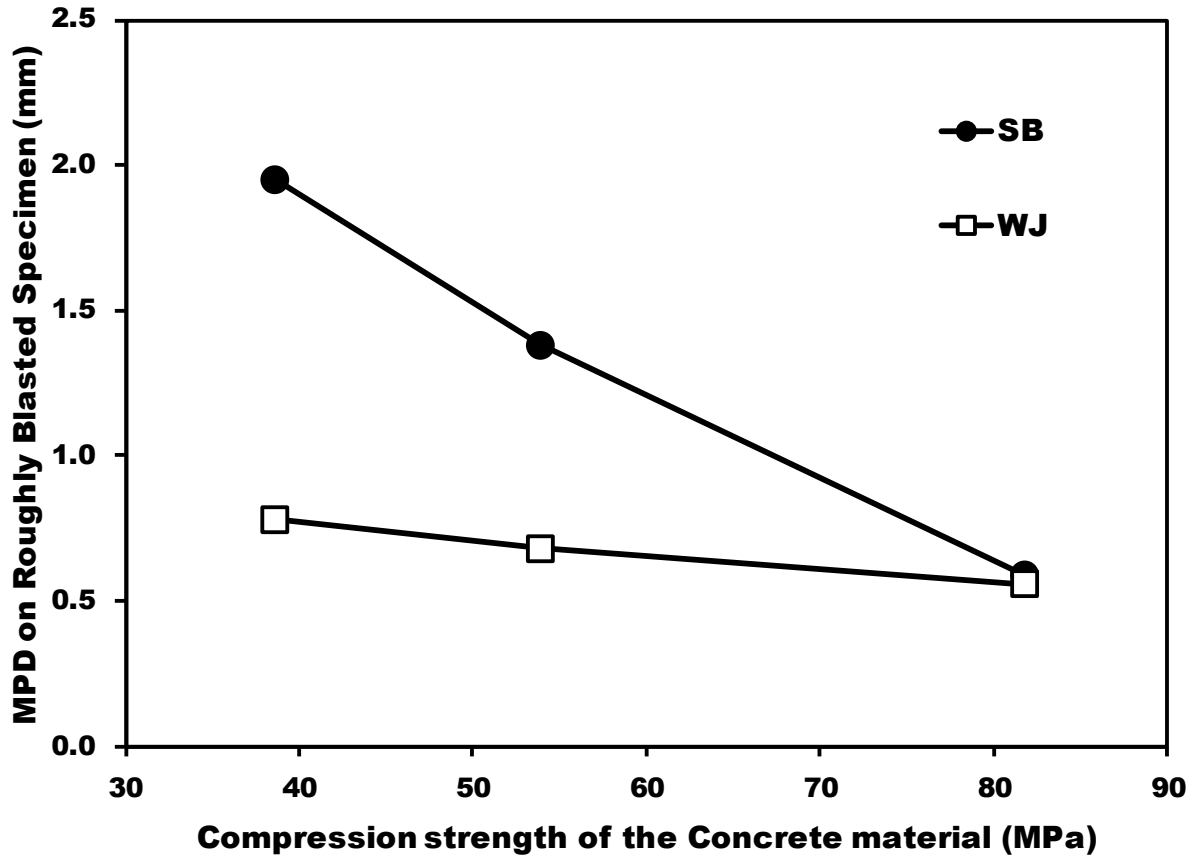
1



2
3
4
5
6

FIGURE 8 Relation MPD, Round Index and μ80(DFT)

1



2
3
4
5
6

FIGURE 9 MPD on roughly blasted specimen by compression strength

1 **TABLE 1 Concrete mix proportion**
2

Mix number	Max size of aggregates (mm)	Water cement ratio (%)	Quantity of material per unit volume of concrete						compressive strength after 28 days (MPa)
			water (kg/m ³)	cement (kg/m ³)	sand (kg/m ³)	coarse aggregate (kg/m ³)	AE (g/m ³)	AE-H (g/m ³)	
No.1	20	45.0	150	334	769	1066	3340	–	38.6
No.2	20	38.5	170	442	700	995	–	4420	53.9
No.3	20	30.1	170	565	730	881	–	8480	81.8

AE : air-entraining and water-reducing admixture

AE-H : air-entraining and high-range water-reducing admixture

3
4
5

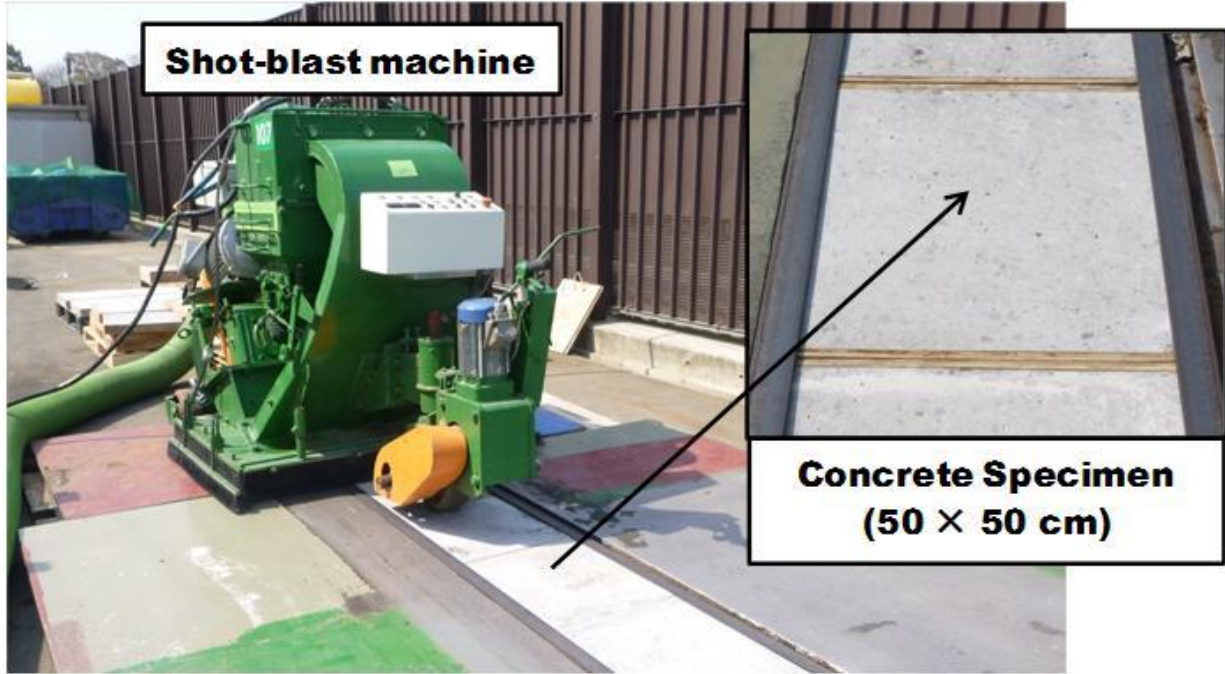
1 **TABLE 2 Conditions of shot-blast (SB) and water-jet (WJ) methods**

2

No.	Conditions					
	SB		WJ			
	Shot Density (kg/m ²)	Steel Diameter (mm)	Hydraulic Pressure (MPa)	Cycle (rpm)	Number of Nozzle (count)	Moving Velocity (m/min)
SB1	150	1.4				
SB2	150	2.0				
SB3	150	2.4				
SB4	200	2.0				
WJ1			230	50	8	2.0
WJ2			245	50	8	2.0
WJ3			245	200	30	2.0
WJ4			245	100	8	1.0

3
4
5

1



2

3

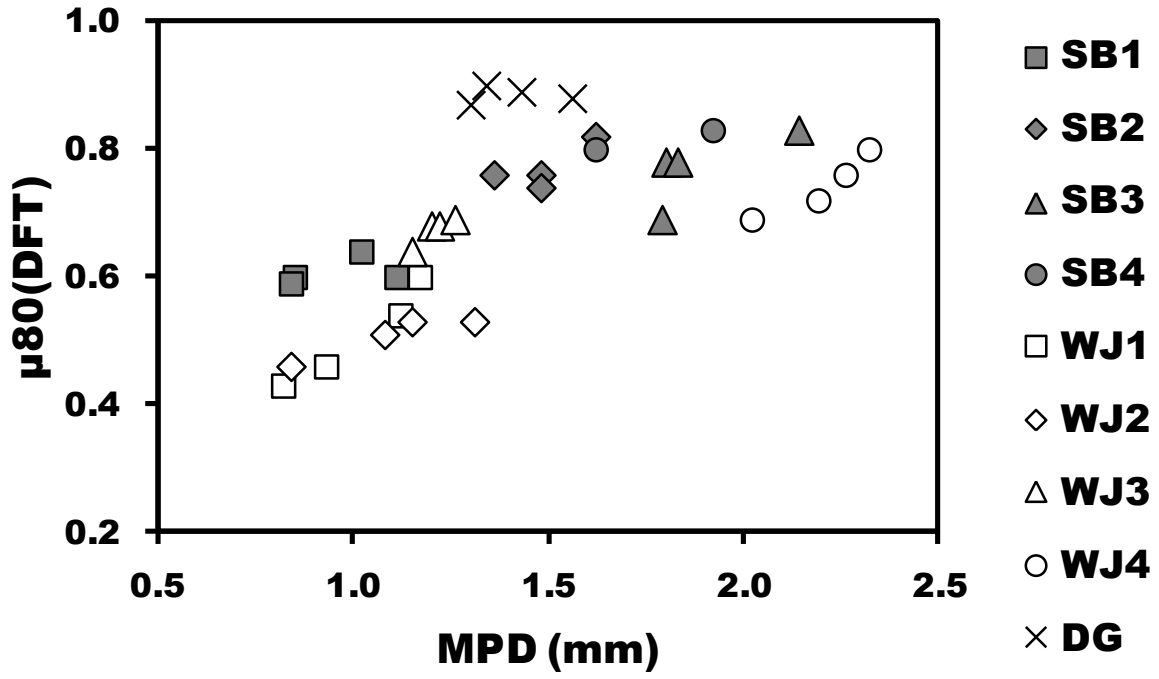
4

5

6

PHOTO 3 Shot-blast testing

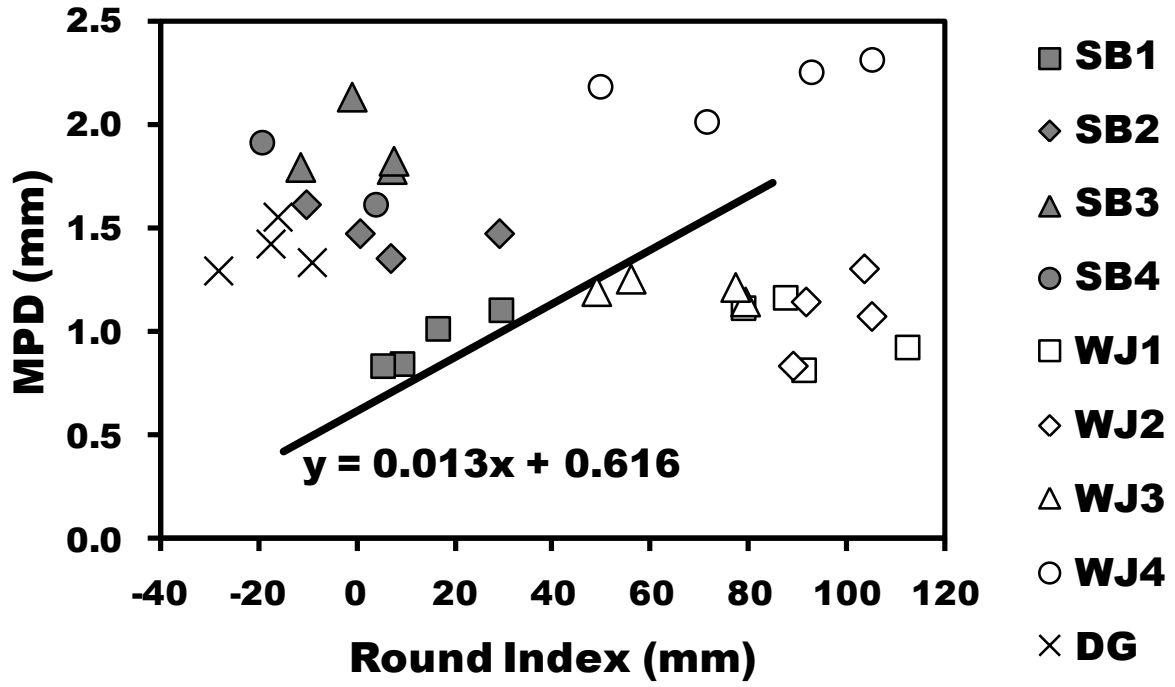
1



2
3
4
5
6

FIGURE 10 $\mu_{80}(\text{DFT})$ and MPD after all skid resistance recovery tests

1



2
3
4
5
6

FIGURE 11 MPD and Round Index after recovery tests

REFERENCES

- 1 1. *Standard Test Method for Measuring Paved Surface Frictional Properties Using the*
2 *Dynamic Friction Tester*. ASTM E1911-98.
- 3 2. Karen L, Scrivener. *Backscattered electron imaging of cementitious microstructures:*
4 *understanding and quantification*. Cement & Concrete Composites 26, 2004
- 5 3. *Standard Test Method for Measuring Pavement Macrotexture Properties Using the*
6 *Circular Track Meter*. ASTM E2157-01. PIARC.
- 7 4. J.W. Hall, K.L. Smith, L.Titus-Glover, J.C. Wambold, T.J. Yager, Z.Rado. *Guide*
8 *for Pavement Friction*. NCHRP, Web-Only Document 108, Transportation
9 Research Board, 2009
- 10 5. PIARC. *Report of the Committee on Surface Characteristics*. Proceedings of the
11 18th World Road Congress, Brussels, 1987
- 12 6. Gunaratne, M., Weerasuriya, S., Chawla, M., and Ulroch, P. *Simulation of Pavement*
13 *Texture for Prediction of Hysteresis Friction*. SAE Technical Paper Series 951417, 1995
- 14 7. Ichihara, K., and Onoda, M. *A skid resistance of road surface and the measure (in*
15 *Japanese)*. GIJYUTSU SYOIN, 1997
- 16 8. Japan Society of Civil Engineers. *Pavement Surface Texture and Skid Resistance*.
17 Pavement Engineering Library 10, 2013
- 18 9. Bernard, I., Izevbekhai., and W. James Wilde. *Innovative Diamond Grinding on MnROAD*
19 *Cells 7, 8, 9, and 37*. Minnesota Department of Transportation Research Services, 2010
- 20
- 21